# Distinct and Non-additive Effects of Urea and Guanidinium Chloride on Peptide-Solvation

Pritam Ganguly[1] and Joan-Emma Shea*[1,2]

[1]*Department of Chemistry and Biochemistry, University of California at Santa Barbara, Santa Barbara, California 93106, USA.*

[2]*Department of Physics, University of California at Santa Barbara, Santa Barbara, California 93106, USA.*

**Abstract**

Using enhanced-sampling replica exchange fully-atomistic molecular dynamics simulations, we show that individually, urea and guanidinium chloride (GdmCl), denature the Trpcage protein, but that remarkably, the helical segment $^{1}$NLYIQWL$^{7}$ of the protein is stabilized in mixed denaturant solutions. GdmCl induces protein denaturation via a combination of direct and indirect effects involving dehydration of the protein and destabilization of stabilizing salt bridges. In contrast, urea denatures the protein through favorable protein-urea preferential interactions, with peptide-specific indirect effects of urea on the water structure around the protein. In the case of the helical segment of Trpcage, urea "over-solvates" the peptide backbone by reorganizing water molecules from the peptide side chains to the peptide backbone. An intricate non-additive thermodynamic balance between GdmCl-induced dehydration of the peptide and the urea-induced changes in solvation structure triggers partial counteraction to urea-denaturation and stabilization of the helix.

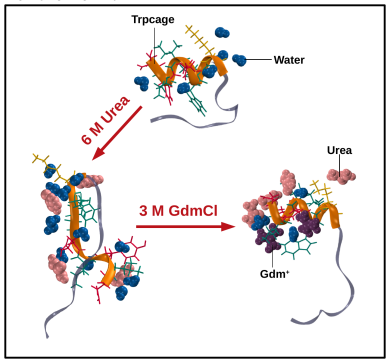


Guanidinium chloride (GdmCl) and urea are two of the most common protein denaturants used in *in vitro* experiments, yet the molecular mechanisms behind GdmCl [1–21] and urea [1,12,22–37] denaturation remain a matter of debate in the literature. The thermodynamic properties of aqueous solutions of urea and GdmCl may not necessarily be additive when mixed. For example, vapor-pressure osmometry measurements of urea-GdmCl mixtures show the non-additivity of the osmotic coefficients of individual urea or GdmCl solutions and suggest favorable interactions between urea and GdmCl.[38] The combined effects of urea and GdmCl on proteins in mixed denaturant conditions and the underlying molecular mechanisms through which urea-GdmCl mixtures interact with proteins remain unclear. The non-additivity of the denaturing effects of these two denaturants have also been reported in MD simulation studies.[39,40] Hydrophobic collapse of Lysozyme,[39] as well as of a hydrophobic polymer,[40] has been reported in mixtures of urea and GdmCl by Zhou and coworkers. It has been reported earlier that mixtures of GdmCl and urea may potentially be less efficient in denaturing Lysozyme than pure urea or GdmCl solutions.[38] Single-molecule spectroscopy experiments have indicated increased hydrophobic interactions in cold shock protein in urea-GdmCl mixture, although a direct collapse has not been observed.[41] In the aforementioned works by Zhou and coworkers, this so-called cononsolvency of proteins in the mixtures of urea and GdmCl has been explained in terms of the GdmCl-induced urea depletion from protein surfaces and the crowding effects of the two denaturants when mixed together. Using scaled particle theory,[42] Graziano has proposed an alternative explanation for the cononsolvency where the higher densities of the urea-GdmCl solutions along with the deficit of the water molecules in the solvation shells of the solutes and the cosolvents have been taken into account.[43] In the context of the cononsolvency of proteins in mixed denaturants, we note that the collapse of polymers in mixtures of "good" solvents has been widely reported in the literature.[44–51]

In order to elucidate the molecular mechanisms behind urea and GdmCl denaturation in pure and mixed denaturant solutions, in this paper, we study two small synthetic peptides, Trpcage (NLYIQWLKDGGPSSGRPPPS)[52–63] and Trpzip1 (SWTWEGNKWTWK),[8,64–66] under different denaturant conditions. Trpcage and Trpzip1 have stable and distinct native structures in aqueous medium at 300 K temperature and the thermal stabilities of these two peptides are comparable in terms of their melting temperatures (317 K for Trpcage[60] and 323 K for Trpzip1[64]). The native conformation of Trpcage in water[52] consists of an $\alpha$-helical segment, a stable salt bridge between the Asp9 and the Arg16 residues, and a hydrophobic core formed by the packing of the Tyr3 and Trp6 residues against the Gly11, Pro12, Pro18 and Pro19 residues (PDB entry 1L2Y). On the other hand, tryptophan zipper peptide Trpzip1, which has a $\beta$-hairpin structure in water,[64] is stabilized in aqueous medium through "zipper"-like stacking of the indole groups of the tryptophan residues (PDB entry 1LE0). Denaturation of Trpcage and Trpzip1 in urea and GdmCl has been reported in the past through MD simulations,[8,27,67,68] as well as through spectroscopic measurements.[8,52,67,69] However, the molecular mechanism of the denaturation, especially in pure GdmCl solutions and mixed urea-GdmCl solutions, remain unclear. Here in this paper, using all-atomistic enhanced-sampling replica-exchange molecular dynamics simulations,[70–72] we systematically study the effects of urea and GdmCl on the structure, solva-

*Corresponding author. E-mail: shea@chem.ucsb.edu

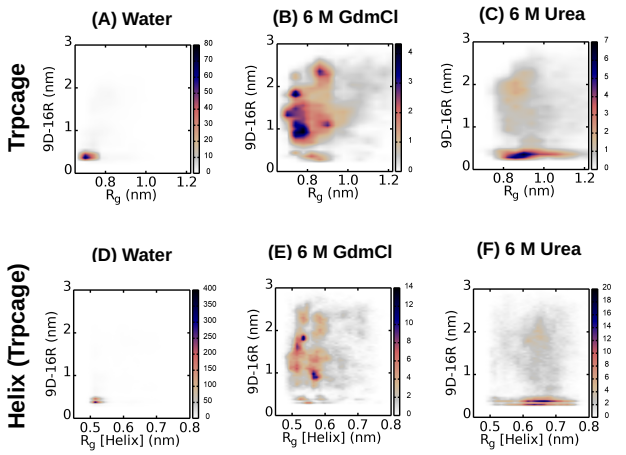


**Figure 1:** (A-C): Plotted are the distributions of the radius of gyration ($R_g$) of Trpcage and the distance ($9D-16R$) between the center of masses of the $COO^-$ and the $H_2NCNH_2^+$ groups of the aspartic acid and the arginine residues respectively in Trpcage for (A) water, (B) 6 M GdmCl, and (C) 6 M urea. (D-F): Plotted are the distributions of the radius of gyration ($R_g[Helix]$) of the $^1$NLYIQWL$^7$ segment of Trpcage and the distance ($9D-16R$) between the center of masses of the $COO^-$ and the $H_2NCNH_2^+$ groups of the aspartic acid and the arginine residues respectively in Trpcage for (D) water, (E) 6 M GdmCl, and (F) 6 M urea.

tion thermodynamics and intra-peptide interactions of Trpcage and Trpzip1 peptides in pure and mixed denaturant conditions. Solvation thermodynamics, in terms of the Kirkwood-Buff integrals (KBIs)[73,74] and the preferential interactions (details can be found in the Supporting Information) of the amino acid monomers with the denaturants, is also reported.

In Trpcage, the salt bridge formed between the aspartic acid residue (9D) and the arginine residue (16R) significantly contributes to the native stability of the protein.[52,75] To investigate the effects of GdmCl and urea on both the 9D-16R salt bridge of Trpcage and the overall compaction or extension of the peptide, we calculate the distributions of the radius of gyration ($R_g$) and the distance between the center of masses of the $COO^-$ and the $H_2NCNH_2^+$ groups of the 9D and the 16R residues respectively (referred to as 9D-16R distance henceforth) in water, 6 M GdmCl and in 6 M urea solutions. The corresponding data are shown in Figure 1(A), 1(B) and 1(C) respectively. In water, the most probable 9D-16R distance has been found to be $<$0.5 nm. In the GdmCl solution, the majority of the populations for the 9D-16R distance has been found at values $\geq$1.0 nm. In the urea solutions, however, the most probable 9D-16R distance is $<$0.5 nm. In water, the most probable $R_g$ for the peptide is $\approx$0.7 nm. In GdmCl, the $R_g$ of the peptide does not increase significantly and a very high population has been found at $<$0.8 nm. In contrast, the corresponding results for the urea solutions show a much broader distribution of $R_g$, with the most probable value for the $R_g$ being $\approx$0.9 nm. In Figure S1 in the Supporting Information, we separately plot the percentage of time when the 9D-16R salt bridge has been identified in the trajectories obtained for Trpcage in different solvent conditions. In 6 M denaturant solutions, the salt bridge is 6 times more likely to form in the presence of urea than of GdmCl. Qualitatively similar results have been observed for Trpzip1. The formation of the 5E-12K salt bridge of Trpzip1 is disfavored in the unfolded configurations and the probability of the formation of the 5E-12K salt bridge in 4 M urea is 5.4 times higher than that in 4 M GdmCl (Figure S2 in the Supporting Information). From the distributions of the intra-peptide hydrogen bonds for Trpcage and Trpzip1 in different solvent conditions, shown in Figures S3 and S4 in the Supporting Information respectively, it may be argued that GdmCl and urea (at equal concentrations) have similar effects in reducing the number of the intra-peptide hydrogen bonds. A picture hence emerges in which GdmCl destabilizes the salt bridges and promotes compact yet denatured structures of the peptides, while urea is seen to be significantly less effective than GdmCl at destabilizing the salt bridges, yet it induces extended denatured structures. Qualitatively, similar results can be found when we calculate the distribution of the $R_g$ of the helical segment ($^1$NLYIQWL$^7$) of Trpcage with the 9D-16R distance (Figure 1D-F) in water, 6 M GdmCl and in 6 M urea solutions.

Interestingly, in the mixed denaturant conditions, we find that the helical segment ($^1$NLYIQWL$^7$) of Trpcage significantly retains its native structure. In Figure 2 we show the distributions of the root-mean-squared-displacement (rmsd, dnoted by $rmsd[Helix]$) of the backbone atoms ($N-C_\alpha-C$) of the $^1$NLYIQWL$^7$ segment of Trpcage from the native conformations and the corresponding radius of gyration ($R_g$, denoted by $R_g[Helix]$) of the segment for Trpcage in water, 6 M urea, 6 M GdmCl, and in the mixture of 6 M urea with 3 M GdmCl. In the mixed 6 M urea and 3 M GdmCl solutions, we find that the most probable $R_g$ ($<$0.4 nm) and rmsd ($<$0.1 nm) correspond to the native-like conformations of the segment. The most probable structures of the $^1$NLYIQWL$^7$ segment of Trpcage in water, 6 M urea, 6 M GdmCl, and in the mixture of 6 M urea with 3 M GdmCl are shown in Figure 3. In this figure, the root-mean-squared-displacement (rmsd) of the backbone atoms ($N-C_\alpha-C$) of only the $^1$NLYIQWL$^7$ segment is used for identifying the clusters of similar conformations. The most probable structure of the $^1$NLYIQWL$^7$ segment of Trpcage in GdmCl solution is seen to be denatured yet compact whereas, in urea, the corresponding most probable structure is extended. As can be seen from the most probable structures of the helical segment shown in Figure 3, the probability of finding the native folded structures in the GdmCl-urea mixture is significantly higher than in pure urea or GdmCl solutions. Hence the addition of 3 M GdmCl to 6 M urea solution partially counteracts the urea-denaturation of the helical segment of Trpcage. Qualitatively similar results are found when 4 M GdmCl is added to 4 M urea solutions (results are shown in Figure S5 in the Supporting Information). However, the counteraction mechanism of GdmCl in the presence of urea is not identified when the $R_g$ and the rmsd of the Trpcage protein as a whole is considered. The distributions of the rmsd of the backbone atoms and the corresponding $R_g$ of the full-length Trpcage in water and denaturants are shown in Figures S6 and S7 in the Supporting Information. The corresponding most probable structures (where the rmsd of the backbone atoms of the full-length Trpcage peptide has been used) are shown in Figures S8 and S9 in the Supporting Information. These results indicate that the counteraction to the urea-denaturation by GdmCl is limited to the helical segment of the Trpcage protein. Also for Trpzip1 (Figures S10 and S11 in the Supporting Information), no effective refolding in mixed urea-GdmCl solutions has been observed.

The enhanced stability of the helical segment of Trpcage in mixed urea-GdmCl solutions, in contrast to the full-length Trpcage and Trpzip1, can be explained by the distributions of the denaturants and the water molecules around the peptide. We start with discussing the effects of the denaturants on the water structures around the peptides. In Figure 4 we have plotted the average number of hydrogen bonds between the helical segment of Trpcage and the solvent water, urea and $Gdm^+$ for Trpcage in pure water, in 4 and 6 M urea

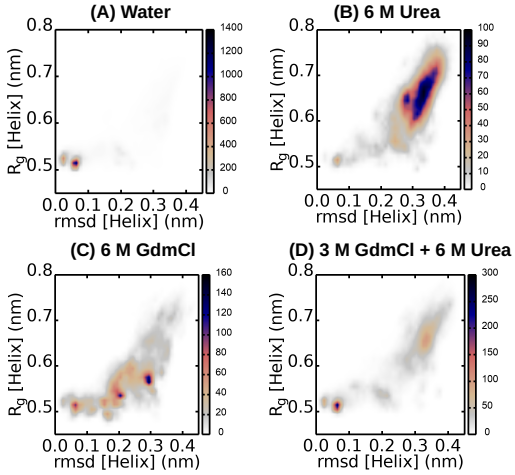


**Figure 2:** Plotted are the distributions of the root-mean-squared-displacement ($rmsd[Helix]$) of the backbone atoms ($\mathrm{N}-\mathrm{C}_\alpha-\mathrm{C}$) of the $^1$NLYIQWL$^7$ segment of Trpcage from the native conformations and the radius of gyration ($R_g[Helix]$) of the aforementioned segment for Trpcage in (A) water, (B) 6 M urea, (C) 6 M GdmCl, and (D) in the mixture of 6 M urea with 3 M GdmCl.

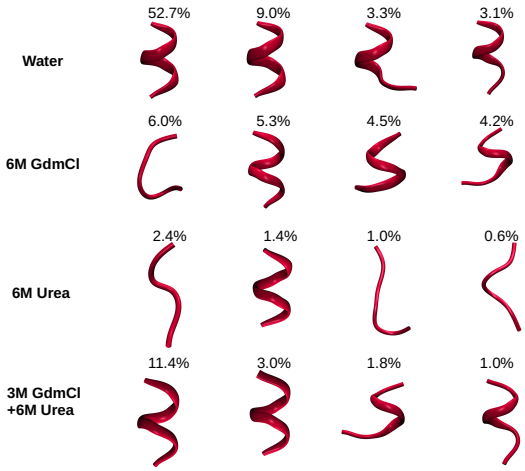


**Figure 3:** Shown are the four most probable conformations of the $^1$NLYIQWL$^7$ segment of Trpcage in water, 4 and 6 M urea, and 4 and 6 M GdmCl. The corresponding probabilities of finding the structures are also reported. The root-mean-squared-displacement (rmsd) of the backbone atoms ($\mathrm{N}-\mathrm{C}_\alpha-\mathrm{C}$) of only the $^1$NLYIQWL$^7$ segment is used for identifying the clusters of the similar conformations.

and in 4 and 6 M GdmCl. The hydrogen bonds are calculated separately for the backbone and the side chain atoms. Our results show that the addition of urea to water increases the number of backbone-water hydrogen bonds but reduces the number of hydrogen bonds between the protein side chains and water. Probing deeper, we next plot the number of water molecules which are within 0.4 nm of the individual amino acid backbone and side chain for each of the amino acids in $^1$NLYIQWL$^7$, in the presence and in absence of 6 M urea. Our results, plotted in Figure S12 (upper panel) in the Supporting Information, show an overall trend for the accumulation of more water molecules around the backbone of $^1$NLYIQWL$^7$, when urea is added to water. Figure S12 (lower panel) in the Supporting Information shows that urea directly depletes water from the side chains of $^1$NLYIQWL$^7$, except for the tryptophan residue. Interestingly, for the tryptophan residue, the addition of urea increases the number of water molecules around both the backbone and the side chain. This can be attributed to the exposure of the tryptophan side chain, buried in the hydrophobic core in water, to the water in the conformations adopted in binary urea-water solvent. Nonetheless, an overall reorganization of the solvent water molecules from the solvation shells of the protein side chains to the solvation shell of the protein backbone can be found in the presence of urea. In contrast, for the other segment of Trpcage ($^8$KDGGPSSGRPPPS$^{20}$), urea has been found to deplete water from the backbone, as well as from the side chains (Figure S13 in the Supporting Information). Similar results are found for Trpzip1 in urea solution (Figure S14 in the Supporting Information) where no reorganization of the water molecules has been identified. GdmCl tends to dehydrate the side chains of the helical segment of Trpcage much effectively than urea (Figure 4). Stronger dehydration of peptide by GdmCl than urea has also been found for Trpzip1 peptide (Figure S14 in the Supporting Information).

Next, we plot the numbers of the denaturants around the amino acid residues, normalized with the solvent accessible surface area (SASA) of the amino acids (results are shown in Figures S15 and S16 in the Supporting Information for Trpcage and Trpzip1 respectively). We find that the accumulation of urea around the peptides is significantly higher than $\mathrm{Gdm}^+$. Our results also show that $\mathrm{Gdm}^+$ does not have any preference for residues with planar groups over others. Using the distributions of water and denaturants around the peptides, in Figure 5 and in Figure S17 in the Supporting Information we plot the preferential interactions (Eq. S6 in the Supporting Information) between the peptides and the denaturants in different solvent conditions. In GdmCl solutions, the peptide-$\mathrm{Gdm}^+$ preferential interactions are close to zero (for both Trpcage and Trpzip1). It must be noted that near-zero peptide-GdmCl preferential interactions have been reported earlier,[17,76] and that peptide-GdmCl preferential interactions depend strongly on the amino acid compositions of the peptides.[77,78] For both peptides, we find that the peptide-urea preferential interactions are significantly higher than the peptide-$\mathrm{Gdm}^+$ preferential interactions. Comparing the results for pure urea or GdmCl solutions with the results in mixed urea-GdmCl solutions, it can be seen that the addition of urea to GdmCl solutions depletes $\mathrm{Gdm}^+$ from the peptides and decreases peptide-$\mathrm{Gdm}^+$ preferential solvation. In contrast, the addition of GdmCl to urea solutions moderately increases urea accumulation around the peptide and also increases the peptide-urea preferential solvation. Further simulations of individual amino acid monomers in the denaturant solutions show, except for negatively charged aspartic acid, positive amino acid-urea KBIs (Eq. S2 in the Supporting Information) and negative amino acid-$\mathrm{Gdm}^+$ KBIs (results are shown in Figure S18 in the Supporting Information). A negative amino acid-$\mathrm{Gdm}^+$ KBI reflects less density of $\mathrm{Gdm}^+$ ions around amino acids than that in their bulk phase. These results show that $\mathrm{Gdm}^+$ does not have favorable interactions with the amino acids studied (except for the negatively charged amino acids).

Taken together, in GdmCl solutions, the total number of solvent molecules is significantly smaller than that in the urea solutions of similar concentrations. The effective solvation of the denatured conformations of the peptide in urea promotes extended structures. In contrast, GdmCl promotes less solvated denatured yet compact structures of the peptide. Qualitatively similar observations have been made in an earlier experimental study (FRET and far-UV CD) where it has been found that GdmCl may favor dehydrated molten glob-

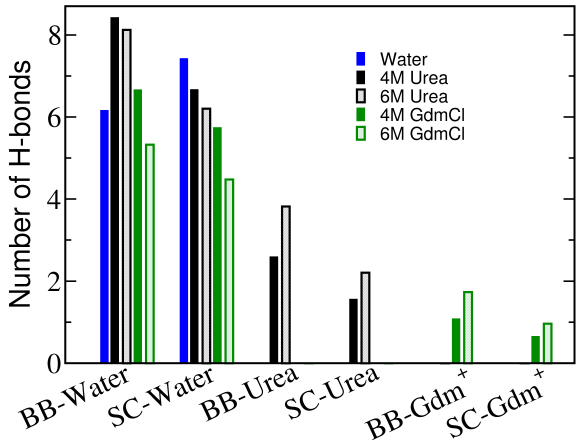


**Figure 4:** Shown are the numbers of hydrogen bonds between the $^{1}$NLYIQWL$^{7}$ segment of Trpcage and solvents (water, $\mathrm{Gdm}^{+}$ and urea). Plotted are the results for water, 6 M urea, 6 M GdmCl and mixture of 6 M urea with 3 M GdmCl. BB: backbone; SC: side chains. The maximum error in the calculations is $< 0.01$.

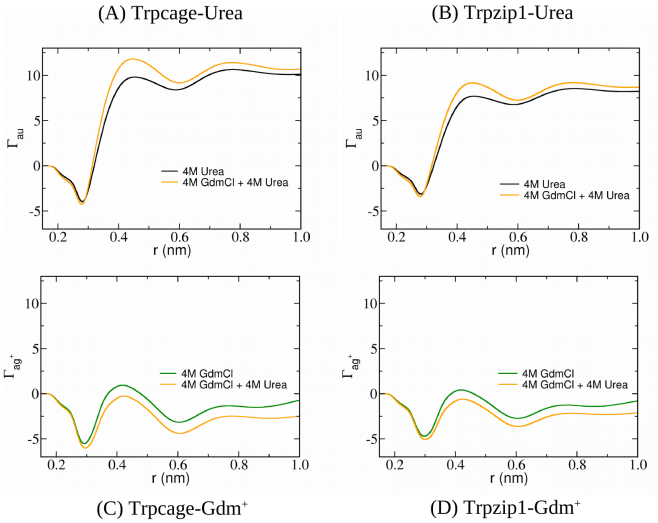


**Figure 5:** Plotted are the preferential interaction of urea with (A) Trpcage and (B) Trpzip1 and of $\mathrm{Gdm}^{+}$ with (C) Trpcage and (D) Trpzip1 for 4 M GdmCl, 4 M urea and the mixture of 4 M GdmCl and 4 M urea. Results are shown as functions of r where r denotes the closest distance between the center of mass of urea or $\mathrm{Gdm}^{+}$ and the surfaces of the peptides.

ule like structures in peptide.[79] Since in pure urea solutions, the extended conformations of the $^{1}$NLYIQWL$^{7}$ peptide segment forms an excess number of backbone-water hydrogen bonds (Figure 4), the GdmCl-induced effective reduction in the number of backbone-water hydrogen bonds may potentially lead to the partial counteraction to the urea-induced denaturation of the helical segment of Trpcage in mixed urea-GdmCl solutions. Comparing the solvation properties of the $^{1}$NLYIQWL$^{7}$ peptide segment in pure GdmCl solutions with the mixed GdmCl-urea solutions it becomes apparent that the dry molten structures of the peptide in pure GdmCl solutions are solvated by urea in mixed denaturant conditions. Thus, in the mixed GdmCl-urea solutions, neither is the peptide backbone "over-solvated" by water and urea as in the pure urea solutions, nor are the peptide side chains "under-solvated" as in pure GdmCl solution. This delicate balance in the peptide-solvent hydrogen bonding properties results into the partial counteraction to the urea- or GdmCl-induced denaturation in the mixed-denaturant solutions. As mentioned earlier, since the formation of additional backbone-water hydrogen bonds in the denatured states of Trpzip1 and the $^{8}$KDGGPSSGRPPPS$^{20}$ segment of Trpcage is not favored in the presence of urea, the GdmCl-induced dehydration of the peptides in the mixtures of urea and GdmCl does not effectively result in counteraction of urea-denaturation in Trpzip1 and the $^{8}$KDGGPSSGRPPPS$^{20}$ segment of Trpcage.

In conclusion, in this paper, we have studied the conformational stability and the solvation thermodynamics of two model peptides, Trpcage and Trpzip1, in presence of pure and mixed urea and GdmCl solutions. The key observations from our study are: A) Urea has been found to preferentially solvate the peptides, thereby denaturing the peptides. In contrast, GdmCl has nearly zero preferential interactions with the peptides studied. GdmCl has been found to denature the peptides through a combined mechanism of peptide-dehydration and salt bridge-destabilization. (B) In mixed denaturant conditions, urea significantly removes $\mathrm{Gdm}^{+}$ ions from the peptide surfaces. In contrast, GdmCl does not deplete urea from the peptide surfaces, rather, it slightly promotes accumulation of urea around the peptides. (C) Interestingly, our results show partial counteraction to urea-denaturation of the helical segment $^{1}$NLYIQWL$^{7}$ of Trpcage by GdmCl, with folded native-like conformations of the segment observed in mixtures of urea and GdmCl. Unlike the cases for Trpzip1 and the $^{8}$KDGGPSSGRPPPS$^{20}$ segment of Trpcage where water molecules are depleted from the backbone in the presence of urea, urea has been found to promote aggregation of water molecules around the backbone of the helical segment $^{1}$NLYIQWL$^{7}$ of Trpcage. As in the cases of Trpzip1 and the $^{8}$KDGGPSSGRPPPS$^{20}$ segment of Trpcage, urea depletes water molecules from the side chains of the $^{1}$NLYIQWL$^{7}$ segment of Trpcage (except for the Trp6 residue). The reorganization of the water molecules from the side chains to the backbone of the $^{1}$NLYIQWL$^{7}$ segment of Trpcage effectively causes "over-hydration" of the peptide. We propose that a delicate balance between GdmCl-induced dehydration and the urea-induced "over-hydration" of the $^{1}$NLYIQWL$^{7}$ segment of Trpcage may lead to the partial counteraction to urea-denaturation by GdmCl.

## SIMULATION DETAILS

All molecular dynamics simulations are carried out using the GROMACS molecular dynamics package (versions 5.1.2, 2016 and 2016.3).[80] Trpcage and Trpzip1 peptides are modeled using the AMBER99SB-ILDN force field[81] with the rigid TIP3P water parameters[82] and the native conformations of the peptides are shown in Figures S8 and S11 in the Supporting Information, respectively. Additional simulations of the peptides have been carried out using the OPLS-AA force field[83–85] with the rigid TIP3P water model. Amino acid monomers are modeled using the AMBER99SB-ILDN force field (with rigid TIP3P water model). Additional simulations for the amino acid monomers are performed using the OPLS-AA with the TIP3P water model and using the GROMOS54A7[86] parameters with the rigid SPC/E model for water.[87] Unless stated otherwise, the results are shown for the AMBER99SB-ILDN peptide force field with the rigid TIP3P water model. The peptides and the amino acid monomers are capped by acetyl group and amide group at the N and the C termini respectively. Urea has been modeled using the Kirkwood-Buff derived Smith urea force field.[88] For GdmCl, a

modified version of the Kirkwood-Buff derived Smith GdmCl force field,[89] derived by Jungwirth and coworkers,[90] has been used. All the van der Waals cross-interactions are calculated using the standard mixing rules for the peptide force fields. Replica-exchange molecular dynamics simulations for the denaturation studies are carried out for 250 ns per replica where 64 replicas spanning a temperature range of 290 K to 490 K have been used. The folding simulations in pure water are performed for 800 ns and 1350 ns per replica for Trpcage and Trpzip1 respectively when the AMBER99SB-ILDN force field is used. The folding of Trpzip1 in pure water with the OPLS-AA force field is simulated for 500 ns per replica. The technical details of the simulations are provided in the Supporting Information. The justifications for our choice of the force fields and the simulation run-lengths are also given in the Supporting Information. The Kirkwood-Buff theory of solutions[73] and the expressions for the preferential solvations[74] are presented in the Supporting Information.

It must be noted that the AMBER99SB-ILDN force field uses the Lorentz-Berthelot combination rule for the van der Waals cross-interactions. In contrast, the Jungwirth GdmCl force field has been developed using the geometric mean combination rule, compatible with the GROMOS54A7 or the OPLS-AA force fields. In separate simulations of 4 M GdmCl solutions without peptides (details are in the Supporting Information), we have found that the GdmCl solutions show high ion-water KBI and low ion-ion KBI when the Lorentz-Berthelot combination rule is used, which yields a significantly high activity derivative (1.98) than experiments (0.86).[89] In order to study the effects of the combination rules for the van der Waals cross-interactions, we have performed additional simulations of Trpzip1 with the OPLS-AA force field and amino acid monomers with the OPLS-AA and the GROMOS54A7 force fields. We have also performed simulations of Trpcage with the AMBER99SB-ILDN force field where we use the geometric mean rule for the ion-ion and the ion-water van der Waals interactions and the Lorentz-Berthelot combination rule for all the other van der Waals interactions. Additional simulations of the alanine monomers in 4 M GdmCl and in the mixture of 4 M urea and 4 M GdmCl are also performed using the AMBER99SB-ILDN force field and the geometric mean combination rule for all the van der Waals cross-interactions. The corresponding results are shown in the Supporting Information. The conclusions drawn from this work have been found to be independent of the combination rule for the van der Waals cross-interactions.

## ACKNOWLEDGMENTS

We acknowledge the computational support from the Extreme Science and Engineering Discovery Environment (XSEDE) through National Science Foundation (NSF) grant number TG-MCA05S027. This work has used the Stampede 2 supercomputer at the Texas Advanced Computing Center at the University of Texas at Austin. J.-E.S. acknowledges the support from the National Science Foundation (NSF Grant MCB-1716956). The Center for Scientific Computing at the California Nanosystems Institute (NSF Grant CNS-0960316) is also acknowledged. The support from the National Institutes of Health (NIH grant R01-GM118560-01A) is acknowledged.

## SUPPORTING INFORMATION AVAILABLE

The theory of solvation thermodynamics used in this work, the technical details of the simulations, the calculations of the activity derivative of GdmCl with different combination rules for the van der Waals cross-interactions, the calculations of the melting temperatures of the peptides, the distributions of the denaturants around the peptides, the most probable structures and the distributions of the rmsd and the radius of gyration of the peptides in different denaturant conditions (obtained with the OPLS-AA and the AMBER99SB-ILDN peptide force fields), the preferential interactions and the partition coefficients of the peptides with the denaturants, the distributions of the intrapeptide hydrogen bonds and peptide-solvent hydrogen bonds for different denaturant conditions, and the Kirkwood-Buff analyses of the amino acid monomers, modeled with the AMBER99SB-ILDN, OPLS-AA and the GROMOS54A7 force fields, in different denaturant conditions, the effects of the combination rules for the van der Waals cross-interactions on the peptide-denaturant preferential interactions, the alanine-denaturant and the denaturant-denaturant radial distribution functions, and the distributions of the rmsd and the radius of gyration of the helical segment of Trpcage, the effects of the initial configuration of the helical segment of Trpcage on its stability in mixed urea-GdmCl solutions.

## REFERENCES

(1) England, J. L.; Haran, G. Role of Solvation Effects in Protein Denaturation: from Thermodynamics to Single Molecules and Back. *Annu. Rev. Phys. Chem.* **2011**, *62*, 257–277.

(2) Mason, P. E.; Neilson, G. W.; Enderby, J. E.; Saboungi, M.-L.; Dempsey, C. E.; MacKerell, A. D.; Brady, J. W. The Structure of Aqueous Guanidinium Chloride Solutions. *J. Am. Chem. Soc.* **2004**, *126*, 11462–11470.

(3) Vazdar, M.; Heyda, J.; Mason, P. E.; Tesei, G.; Allolio, C.; Lund, M.; Jungwirth, P. Guanidinium Like-Charge Ion Pairing from Aqueous Salts to Cell Penetrating Peptides. *Acc. Chem. Res.* **2018**, *51*, 1455–1464.

(4) Vazdar, M.; Vymětal, J.; Heyda, J.; Vondrášek, J.; Jungwirth, P. Like-Charge Guanidinium Pairing from Molecular Dynamics and Ab Initio Calculations. *J. Phys. Chem. A* **2011**, *115*, 11193–11201.

(5) Vazdar, M.; Uhlig, F.; Jungwirth, P. Like-Charge Ion Pairing in Water: An Ab Initio Molecular Dynamics Study of Aqueous Guanidinium Cations. *J. Phys. Chem. Lett.* **2012**, *3*, 2021–2024.

(6) Mason, P. E.; Brady, J. W.; Neilson, G. W.; Dempsey, C. E. The Interaction of Guanidinium Ions with a Model Peptide. *Biophys. J.* **2007**, *93*, L04–L06.

(7) Kubíčková, A.; Křížek, T.; Coufal, P.; Wernersson, E.; Heyda, J.; Jungwirth, P. Guanidinium Cations Pair with Positively Charged Arginine Side Chains in Water. *J. Phys. Chem. Lett.* **2011**, *2*, 1387–1389.

(8) Dempsey, C. E.; Piggot, T. J.; Mason, P. E. Dissecting Contributions to the Denaturant Sensitivities of Proteins. *Biochemistry* **2005**, *44*, 775–781.

(9) Dempsey, C. E.; Mason. P. E.; Jungwirth, P. Complex Ion Effects on Polypeptide Conformational Stability: Chloride and Sulfate Salts of Guanidinium and Tetrapropylammonium. *J. Am. Chem. Soc.* **2011**, *133*, 7300–7303.

(10) Mason, P. E.; Dempsey, C. E.; Neilson, G. W.; Kline, S. R.; Brady, J. W. Preferential Interactions of Guanidinum Ions with Aromatic Groups over Aliphatic Groups. *J. Am. Chem. Soc.* **2009**, *131*, 16689–16696.

(11) Ding, B.; Mukherjee, D.; Chen, J.; Gai, F. Do Guanidinium and Tetrapropylammonium Ions Specifically Interact with Aromatic Amino Acid Side Chains? *Proc. Natl. Acad. Sci. U.S.A.* **2017**, *114*, 1003–1008.

(12) O'Brien, E. P.; Dima, R.; Brooks, B.; Thirumalai, D. Interactions between Hydrophobic and Ionic Solutes in Aqueous Guanidinium Chloride and Urea Solutions: Lessons for Protein Denaturation Mechanism. *J. Am. Chem. Soc.* **2007**, *129*, 7346–7353.

(13) Ma, C. D.; Wang, C.; Acevedo-Vélez, C.; Gellman, S. H.; Abbott, N. L. Modulation of Hydrophobic Interactions by Proximally Immobilized Ions. *Nature* **2015**, *517*, 347–350.

(14) Godawat, R.; Jamadagni, S. N.; Garde, S. Unfolding of Hydrophobic Polymers in Guanidinium Chloride Solutions. *J. Phys. Chem. B* **2010**, *114*, 2246–2254.

(15) Macdonald, R. D.; Khajehpour, M. Effects of the Protein Denaturant Guanidinium Chloride on Aqueous Hydrophobic Contact-pair Interactions. *Biophys. Chem.* **2015**, *196*, 25–32.

(16) Zheng, W.; Borgia, A.; Buholzer, K.; Grishaev, A.; Schuler, B.; Best, R. B. Probing the Action of Chemical Denaturant on an Intrinsically Disordered Protein by Simulation and Experiment. *J. Am. Chem. Soc.* **2016**, *138*, 11702–11713.

(17) Heyda, J.; Okur, H. I.; Hladílková, J.; Rembert, K. B.; Hunn, W.; Yang, T.; Dzubiella, J.; Jungwirth, P.; Cremer, P. S. Guanidinium can both Cause and Prevent the Hydrophobic Collapse of Biomacromolecules. *J. Am. Chem. Soc.* **2017**, *139*, 863–870.

(18) Lim, W. K.; Rösgen, J.; Englander, S. W. Urea, but not Guanidinium, Destabilizes Proteins by Forming Hydrogen Bonds to the Peptide Group. *Proc. Natl. Sci. Acad. U.S.A.* **2009**, *106*, 2595–2600.

(19) Meuzelaar, H.; Panman, M. R.; Woutersen, S. Guanidinium-Induced Denaturation by Breaking of Salt Bridges. *Angew. Chem. Int. Ed.* **2015**, *54*, 15255–15259.

(20) Biswas, B.; Muttathukattil, A. N.; Reddy, G.; Singh, P. C. Contrasting Effects of Guanidinium Chloride and Urea on the Activity and Unfolding of Lysozyme. *ACS Omega* **2018**, *3*, 14119–14126.

(21) Chen, S.; Itoh, Y.; Masuda, T.; Shimizu, S.; Zhao, J.; Ma, J.; Nakamura, S.; Okuro, K.; Noguchi, H.; Uosaki, K.; Aida, T. Subnanoscale Hydrophobic Modulation of Salt Bridges in Aqueous Media. *Science* **2015**, *348*, 555–559.

(22) Wang, A.; Bolen, D. W. A Naturally Occurring Protective System in Urea-Rich Cells: Mechanism of Osmolyte Protection of Proteins against Urea Denaturation. *Biochemistry* **1997**, *36*, 9101–9108.

(23) Auton, M.; Holthauzen, L. M. F.; Bolen, D. W. Anatomy of Energetic Changes Accompanying Urea-induced Protein Denaturation. *Proc. Natl. Acad. Sci. U.S.A.* **2007**, *104*, 15317–15322.

(24) Klimov, D. K.; Straub, J. E.; Thirumalai, D. Aqueous Urea Solution Destabilizes $\mathrm{A}\beta_{1622}$ Oligomers. *Proc. Natl. Sci. Acad. U.S.A.* **2004**, *101*, 14760–14765.

(25) Rossky, P. J. Protein Denaturation by Urea: Slash and Bond. *Proc. Natl. Acad. Sci. U.S.A.* **2008**, *105*, 16825–16826.

(26) Hua, L.; Zhou, R. H.; Thirumalai, D.; Berne, B. J. Urea Denaturation by Stronger Dispersion Interactions with Proteins than Water Implies a 2-stage Unfolding. *Proc. Natl. Acad. Sci. U.S.A.* **2008**, *105*, 16928–16933.

(27) Canchi, D. R.; Paschek, D.; García, A. Equilibrium Study of Protein Denaturation by Urea. *J. Am. Chem. Soc.* **2010**, *132*, 2338–2344.

(28) Guinn, E. J.; Pegram, L. M.; Capp, M. W.; Pollock, M. N.; Record, M. T. Quantifying Why Urea is a Protein Denaturant, Whereas Glycine Betaine is a Protein Stabilizer. *Proc. Natl. Acad. Sci.* **2011**, *108*, 16932–16937.

(29) Moeser, B.; Horinek, D. Unified Description of Urea Denaturation: Backbone and Side Chains Contribute Equally in the Transfer Model. *J. Phys. Chem. B* **2014**, *118*, 107–114.

(30) Wetlaufer, D. B.; Malik, S. K.; Stoller, L.; Coffin, R. L. Nonpolar Group Participation in the Denaturation of Proteins by Urea and Guanidinium Salts. Model Compound Studies. *J. Am. Chem. Soc.* **1964**, *86*, 508–514.

(31) Roseman, M.; Jencks, W. P. Interactions of Urea and Other Polar Compounds in Water. *J. Am. Chem. Soc.* **1975**, *97*, 631–640.

(32) Ikeguchi, M.; Nakamura, S.; Shimizu, K. Molecular Dynamics Study on Hydrophobic Effects in Aqueous Urea Solutions. *J. Am. Chem. Soc.* **2001**, *123*, 677–682.

(33) Shimizu, S.; Chan. H. S. Origins of Protein Denatured State Compactness and Hydrophobic Clustering in Aqueous Urea: Inferences from Nonpolar Potentials of Mean Force. *Proteins: Struct., Funct., Bioinf.* **2002**, *49*, 560–566.

(34) Bennion, B. J.; Daggett, V. The Molecular Basis for the Chemical Denaturation of Proteins by Urea. *Proc. Natl. Acad. Sci. U.S.A.* **2003**, *100*, 5142–5147.

(35) Trzesniak, D.; van der Vegt, N. F. A.; van Gunsteren, W. F. Computer Simulation Studies on the Solvation of Aliphatic Hydrocarbons in 6.9 M Aqueous Urea Solution. *Phys. Chem. Chem. Phys.* **2004**, *6*, 697–702.

(36) Lee, M.-E.; van der Vegt, N. F. A. Does Urea Denature Hydrophobic Interactions? *J. Am. Chem. Soc.* **2006**, *128*, 4948–4949.

(37) Zangi, R.; Zhou, R.; Berne, B. J. Ureas Action on Hydrophobic Interactions. *J. Am. Chem. Soc.* **2009**, *131*, 1535–1541.

(38) Lilley, T. H.; Tester, D. R. Osmotic Coefficients of Urea Guanidinium Chloride Mixtures in Water at 298.15 K. *J. Chem. Soc., Faraday Trans. 1* **1982**, *78*, 2275–2278.

(39) Xia, Z.; Das, P.; Shakhnovich, E. I.; Zhou, R. Collapse of Unfolded Proteins in a Mixture of Denaturants. *J. Am. Chem. Soc.* **2012**, *134*, 18266–18274.

(40) Das, P.; Xia, Z.; Zhou, R. Collapse of a Hydrophobic Polymer in a Mixture of Denaturants. *Langmuir* **2013**, *29*, 4877–4882.

(41) Hofmann, H.; Nettels, D.; Schuler, B. Single-molecule Spectroscopy of the Unexpected Collapse of an Unfolded Protein at Low pH. *J. Chem. Phys.* **2013**, *139*, 121930.

(42) Lebowitz, J. L.; Helfand, E.; Praestgaard, E. Scaled Particle Theory of Fluid Mixtures. *J. Chem. Phys.* **1965**, *43*, 774.

(43) Graziano, G. An Alternative Explanation for the Collapse of Unfolded Proteins in an Aqueous Mixture of Urea and Guanidinium Chloride. *Chem. Phys. Lett.* **2014**, *612*, 313–317.

(44) Zhang, G.; Wu, C. The Water/Methanol Complexation Induced Reentrant Coil-to-Globule-to-Coil Transition of Individual Homopolymer Chains in Extremely Dilute Solution. *J. Am. Chem. Soc.* **2001**, *123*, 1376–1380.

(45) Schild, H. G.; Muthukumar, M.; Tirrell, D. A. Cononsolvency in Mixed Aqueous Solutions of Poly(N-isopropylacrylamide). *Macromolecules* **1991**, *24*, 948–952.

(46) Wolf, B. A.; Willms, M. M. Measured and Calculated Solubility of Polymers in Mixed Solvents: Co-nonsolvency. *Makromol. Chem.* **1978**, *179*, 2265–2277.

(47) Grosberg, A. Y.; Erukhimovich, I. Y.; Shakhnovich, E. I. On DNA Compaction in Diluted Polymeric Solutions. *Biofizika* **1981**, *26*, 415–420.

(48) Grosberg, A. Y.; Erukhimovitch, I. Y.; Shakhnovitch, E. I. On the Theory of $\Psi$condensation. *Biopolymers* **1982**, *21*, 2413–2432.

(49) Finkelstein, A. V.; Shakhnovich, E. I. Theory of Cooperative Transitions in Protein Molecules. II. Phase Diagram for a Protein Molecule in Solution. *Biopolymers* **1989**, *28*, 1681–1694.

(50) Maccarrone, S.; Scherzinger, C.; Holderer, O.; Lindner, P.; Sharp, M.; Richtering, W.; Richter, D. Cononsolvency Effects on the Structure and Dynamics of Microgels. *Macromolecules* **2014**, *47*, 5982–5988.

(51) Dalgicdir, C.; Rodríguez-Ropero, F.; van der Vegt, N. F. A. Computational Calorimetry of PNIPAM Cononsolvency in Water/Methanol Mixtures. *J. Phys. Chem. B* **2017**, *121*, 7741–7748.

(52) Neidigh, J. W.; Fesinmeyer, R. M.; Andersen, N. H. Designing a 20-residue Protein. *Nature Struct. Biol.* **2002**, *9*, 425–430.

(53) Qiu, L.; Pabit, S. A.; Roitberg, A. E.; Hagen, S. J. Smaller and Faster: The 20-Residue Trp-Cage Protein Folds in 4 $\mu$s. *J. Am. Chem. Soc.* **2002**, *124*, 12952–12953.

(54) Snow, C. D.; Zagrovic, B.; Pande, V. S. The Trp Cage: Folding Kinetics and Unfolded State Topology via Molecular Dynamics Simulations. *J. Am. Chem. Soc.* **2002**, *124*, 14548–14549.

(55) Pitera, J. W.; Swope, W. Understanding Folding and Design: Replica-Exchange Simulations of "Trp-cage" Miniproteins. *Proc. Natl. Acad. Sci. U.S.A.* **2003**, *100*, 7587–7592.

(56) Ahmed, Z.; Beta, I. A.; Mikhonin, A. V.; Asher, S. A. UV-Resonance Raman Thermal Unfolding Study of Trp-Cage Shows That It Is Not a Simple Two-State Miniprotein. *J. Am. Chem. Soc.* **2005**, *127*, 10943–10950.

(57) Neuweiler, H.; Doose, S.; Sauer, M. A Microscopic View of Miniprotein Folding: Enhanced Folding Efficiency through Formation of an Intermediate. *Proc. Natl. Acad. Sci. U.S.A.* **2005**, *102*, 16650–16655.

(58) Juraszek, J.; Bolhuis, P. G. Sampling the Multiple Folding Mechanisms of Trp-cage in Explicit Solvent. *Proc. Natl. Sci. Acad.* **2006**, *103*, 15859–15864.

(59) Paschek, D.; Nymeyer, H.; García, A. E. Replica Exchange Simulation of Reversible Folding/Unfolding of the Trp-cage Miniprotein in Explicit Solvent: On the Structure and Possible Role of Internal Water. *J. Struct. Biol.* **2007**, *157*, 524–533.

(60) Streicher, W. W.; Makhatadze, G. I. Unfolding Thermodynamics of Trp-Cage, a 20 Residue Miniprotein, Studied by Differential Scanning Calorimetry and Circular Dichroism Spectroscopy. *Biochemistry* **2007**, *46*, 2876–2880.

(61) Ryan, D.; Paschek, D.; García, A. E. Microsecond Simulations of the Folding/Unfolding Thermodynamics of the Trp-cage Miniprotein. *Proteins: Struct., Funct., Bioinf.* **2010**, *78*, 1889–1899.

(62) Levine, Z. A.; Fischer, S. A.; Shea, J.-E.; Pfaendtner, J. Trp-Cage Folding on Organic Surfaces. *J. Phys. Chem. B* **2015**, *119*, 10417–10425.

(63) Su, Z.; Mahmoudinobar, F.; Dias, C. L. Effects of Trimethylamine-N-oxide on the Conformation of Peptides and its Implications for Proteins. *Phys. Rev. Lett.* **2017**, *119*, 108102.

(64) Cochran, A. G.; Skelton, N. J.; Starovasnik, M. A. Tryptophan Zippers: Stable, Monomeric $\beta$-hairpins. *Proc. Natl. Acad. Sci. U.S.A.* **2001**, *98*, 5578–5583.

(65) Hayre, N. R.; Singh, R. R. P.; Cox, D. L. Evaluating Force Field Accuracy with Long-time Simulations of a $\beta$-hairpin Tryptophan Zipper Peptide. *J. Chem. Phys.* **2011**, *134*, 035103.

(66) Zerze, G. H.; Uz, B.; Mittal, J. Folding Thermodynamics of $\beta$-hairpins Studied by Replica-Exchange Molecular Dynamics Simulations. *Proteins: Struct., Funct., Bioinf.* **2015**, *83*, 1307–1315.

(67) Heyda, J.; Kožíšek, M.; Bednárova, L.; Thompson, G.; Konvalinka, J.; Vondrášek, J.; Jungwirth, P. Urea and Guanidinium Induced Denaturation of a Trp-Cage Miniprotein. *J. Phys. Chem. B* **2011**, *115*, 8910–8924.

(68) Zheng, W.; Borgia, A.; Borgia, M. B.; Schuler, B.; Best, R. B. Empirical Optimization of Interactions between Proteins and Chemical Denaturants in Molecular Simulations. *J. Chem. Theory Comput.* **2015**, *11*, 5543–5553.

(69) Wafer, L. N. R.; Streicher, W. W.; Makhatadze, G. I. Thermodynamics of the Trp-cage Miniprotein Unfolding in Urea. *Proteins: Struct., Funct., Bioinf.* **2010**, *78*, 1376–1381.

(70) Hukushima, K.; Nemoto, K. Exchange Monte Carlo Method and Application to Spin Glass Simulations. *J. Phys. Soc. Jpn.* **1996**, *65*, 1604–1608.

(71) Sugita, Y.; Okamoto, Y. Replica-exchange Molecular Dynamics Method for Protein Folding. *Chem. Phys. Lett.* **1999**, *314*, 141–151.

(72) Patriksson, A.; van der Spoel, D. A Temperature Predictor for Parallel Tempering Simulations. *Phys. Chem. Chem. Phys.* **2008**, *10*, 2073–2077.

(73) Kirkwood, J. G.; Buff, F. P. The Statistical Mechanical Theory of Solutions. I. *J. Chem. Phys.* **1951**, *19*, 774.

(74) Ben-Naim, A. *Molecular Theory of Solutions*; Oxford University Press: New York, 2006.

(75) Hudáky, P.; Stráner, P.; Farkas, V.; Váradi, G.; Tóth, G.; Perczel, A. Cooperation between a Salt Bridge and the Hydrophobic Core Triggers Fold Stabilization in a Trp-Cage Miniprotein. *Biochemistry* **2008**, *47*, 1007–1016.

(76) Camilloni, C.; Rocco, A. G.; Eberini, I.; Gianazza, E.; Broglia, R. A.; Tiana, G. Urea and Guanidinium Chloride Denature Protein L in Different Ways in Molecular Dynamics Simulations. *Biophys. J.* **2008**, *94*, 4654–4661.

(77) Schneider, C. P.; Trout, B. L. Investigation of Cosolute-Protein Preferential Interaction Coefficients: New Insight into the Mechanism by Which Arginine Inhibits Aggregation. *J. Phys. Chem. B* **2009**, *113*, 2050–2058.

(78) Shukla, D.; Shinde, C.; Trout, B. L. Molecular Computations of Preferential Interaction Coefficients of Proteins. *J. Phys. Chem. B* **2009**, *113*, 12546–12554.

(79) Jha, S. K.; Marqusee, S. Kinetic Evidence for a Two-stage Mechanism of Protein Denaturation by Guanidinium Chloride. *Proc. Natl. Sci. Acad. U.S.A.* **2014**, *111*, 4856–4861.

(80) Hess, B.; Kutzner, C.; van der Spoel, D.; Lindahl, E. GROMACS 4: Algorithms for Highly Efficient, Load-Balanced, and Scalable Molecular Simulation. *J. Chem. Theory Comput.* **2008**, *4*, 435–447.

(81) Lindorff-Larsen, K.; Piana, S.; Palmo, K.; Maragakis, P.; Klepeis, J. L.; Dror, R. O.; Shaw, D. E. Improved Side-Chain Torsion Potentials for the Amber FF99sb Protein Force Field. *Proteins: Struct., Funct., Genet.* **2010**, *78*, 1950–1958.

(82) Jorgensen, W. L.; Chandrasekhar, J.; Madura, J. D.; Impey, R. W.; Klein, M. L. Comparison of Simple Potential Functions for Simulating Liquid Water. *J. Chem. Phys.* **1983**, *79*, 926.

(83) Jorgensen, W. L.; Maxwell, D. S.; Tirado-Rives, J. Development and Testing of the OPLS All-Atom Force Field on Conformational Energetics and Properties of Organic Liquids. *J. Am. Chem. Soc.* **1996**, *118*, 11225–11236.

(84) Rizzo, R. C.; Jorgensen, W. L. OPLS All-Atom Model for Amines: Resolution of the Amine Hydration Problem. *J. Am. Chem. Soc.* **1999**, *121*, 4827–4836.

(85) Kaminski, G. A.; Friesner, R.; Tirado-Rives, J.; Jorgensen, W. L.; Evaluation and Reparametrization of the OPLS-AA Force

Field for Proteins via Comparison with Accurate Quantum Chemical Calculations on Peptides. *J. Phys. Chem. B* **2001**, *105*, 6474–6487.

(86) Schmid, N.; Eichenberger, A. P.; Choutko, A.; Riniker, S.; Winger, M.; Mark, A. E.; van Gunsteren, W. F. Definition and Testing of the GROMOS Force-field Versions 54A7 and 54B7. *Eur. Biophys. J.* **2011**, *40*, 843–856.

(87) Berendsen, H. J. C.; Grigera, J. R.; Straatsma, T. P. The Missing Term in Effective Pair Potentials. *J. Phys. Chem.* **1987**, *91*, 6269–6271.

(88) Weerasinghe, S.; Smith, P. E. A Kirkwood-Buff Derived Force Field for Mixtures of Urea and Water. *J. Phys. Chem. B* **2003**, *107*, 3891–3898.

(89) Weerasinghe, S.; Smith, P. E. A Kirkwood-Buff Derived Force Field for the Simulation of Aqueous Guanidinium Chloride Solutions. *J. Chem. Phys.* **2004**, *121*, 2180.

(90) Wernersson, E.; Heyda, J.; Vazdar, M.; Lund, M.; Mason, P. E.; Jungwirth, P. Orientational Dependence of the Affinity of Guanidinium Ions to the Water Surface. *J. Phys. Chem. B* **2011**, *115*, 12521–12526.